Particle-Gas Dispersion Effects in Confined Coaxial Jets

The objective of this study was to determine the mixing characteristics of two-phase, confined, coaxial jets. Gas composition, gas velocity, and particle mass flux radial profiles were obtained at different axial stations using 20% by weight of 6 or 30 μm spherical aluminum particles in the primary stream. Additional tests were conducted without particles. Radial profiles for gas composition, velocity, and particle flux were correlated using the principle of similarity. In the gas phase, mass mixed more rapidly than momentum, and the 6 μm particles mixed less rapidly than mass or momentum. Systems with low primary density and low secondary velocity mixed most rapidly. An implicit numerical model was developed to predict the rate of mixing of the gas/particle mixture. The model included coupled dynamic and thermal nonequilibrium effects between the gas and solid phases. Comparisons of model predictions and experimental results were good.

PAUL O. HEDMAN

and

L. DOUGLAS SMOOT

Chemical Engineering Department
Brigham Young University
Provo, Utah 84601

SCOPE

Many chemical processes utilize separate streams which mix and often react in a vessel. A common method of contacting these streams is to allow them to exhaust from two coaxial jets into a mixing zone. The jets may be either free (that is, exhausting into an unconfined environment) or confined by the vessel walls.

The considerable effort expended in characterizing the mixing behavior of gaseous free and confined jets has been reviewed by Stowell and Smoot (1973). The mixing process is substantially more complicated, however, when either of the jet streams contains a significant fraction of a particulate phase. Only limited data exist which characterize the mixing of the particulate phase or the effect of the particulate phase on the mixing characteristics of the gaseous phases.

The purpose of this research effort was to determine the mixing characteristics of the gaseous and particulate phases of a central primary jet as it mixes with a clean, gaseous secondary jet. The radial profiles of gas composition, gas velocity, and particle mass flux were measured across the mixing zone at various axial positions downstream from the jet exit. Effects of variation in velocity and density of the streams were also examined.

The facility utilized high pressure air from a reservoir to supply both the primary and secondary jets. In addition, helium and an aluminum powder were introduced into the electrically heated primary jet. Fine-mesh screens were installed near the exit of both the primary and secondary jets to flatten the exit velocity profiles. Existing instrumentation techniques were adapted to measure the helium composition, gas velocity, and particle mass flux. Mixing experiments were conducted at various secondary to primary mass flow ratios (2.6 to 42), secondary to primary density ratios (1 to 4), and secondary to primary velocity ratios (0.1 to 0.45). Tests were conducted without particles, and with 6 and 30 μm spherical aluminum particles in the primary stream.

A computer model was developed using implicit numerical techniques to predict the behavior of a two-phase primary jet mixing with a secondary confined coaxial jet. The model considers gas composition effects as well as fully-coupled, dynamic, and thermal nonequilibrium effects between the gas and particle phases. The mixing is influenced by both turbulent diffusion and nonequilibrium, aerodynamic drag forces. Comparisons between the model predictions and the experimental measurements were reasonable.

CONCLUSIONS AND SIGNIFICANCE

The radial profile data obtained for helium composition, gas velocity, and particle mass flux were each correlated with an empirical dimensionless similar profile. While the similar profile concept for gas composition and velocity data is well documented, the observation of a similar profile for a particulate phase substantially out of equilibrium with the gas has not been previously reported. In the gas phase, the momentum mixed more slowly than did the mass (helium), as noted by many previous investigators. The influence of 20% by weight of either 6 or 30 μm particles in the primary stream on helium and momentum mixing rates was small, the effect on momentum being slightly greater than on mass.

The influence of gas velocity and density variations on the mixing rate was approximately the same for helium composition, gas velocity, and particle mass flux. Increasing the secondary/primary mass flow ratio at a fixed

Correspondence concerning this paper should be addressed to L. D. Smoot. P. O. Hedman is with Tetra Tech, Inc., Arlington, Virginia 22209.

density ratio caused a reduction in jet mixing rate. A low density primary mixed much more rapidly than a high density primary. The enhanced mixing associated with a low density primary was more pronounced with a low secondary velocity than with a high secondary velocity. The greatest mixing occurred when operating with a low-velocity secondary jet and a low-density primary jet.

The Keller and Cebeci (1971) implicit numerical procedure was used for the simultaneous solution of the large number of partial differential equations required for the particle-laden confined jet model. The model predicted the behavior of the helium composition, gas velocity, and 6-μm aluminum powder mass flux within the limits imposed by the particular correlations chosen for gas and particle eddy viscosity. Generally, however, the predicted core length was somewhat shorter than that observed experimentally.

A particle diffusion term based on concentration gradient was included in the model particle continuity equation in order to explain the observed 6-μm particle dispersion rates. This term was found to dominate the predicted powder dispersion process. The predicted behavior of the 30-μm powder was much different from that observed. While the model predicted that essentially no dispersion would occur with the 30-μm powder, the observed dispersion rate was equal to or greater than that observed with the 6-μm powder. Subsequent work (Allred, 1974) has shown that the more rapid dispersion of the larger powder was caused by an excessive initial particle lag with respect to the gas.

Based on the observations drawn from the theoretical predictions for the 6 μm tests, it was concluded that the radial dispersion of the powder was not significantly affected by the gas-particle drag forces. The coupled particle nonequilibrium effects had a small but predictable effect on the dispersion of helium composition and gas velocity. This result was in general agreement with experimental observations.

EXPERIMENTAL PROGRAM

Literature Review

Review of jet mixing literature was reported in an earlier study related to air-breathing combustion processes (Smoot et al., 1969). More recent reviews of the available jet mixing data for gaseous systems have been reported in order to obtain improved mixing predictions (Tufts and Smoot, 1971, Harsha, 1971; Stowell and Smoot, 1973). Fundamental literature for mixing of particle-laden streams is very limited, however. Sargent et al. (1967, 1968) have experimentally investigated the mixing and combustion of reacting, particle-laden streams. Longwell and Weiss (1953) have studied the mixing and distribution of liquid droplets in high-velocity air streams. Goldschmidt and Eskinazi (1966) measured velocity droplet concentrations of μm-size aerosol particles in a plane jet mixing with a secondary stream. Pritts (1970) obtained some nonreactive profile data with 1 μm boron, 50 μm glass beads, and 5.6 and 47.8 μm aluminum particles. Nonuniform particle injection rates, electrostatic charge problems, and nonisokinetic sampling techniques caused the results of Pritts to be in question, however. Field et al. (1966) has reviewed jet mixing related to pulverized coal combustion, including some work for particle-laden jets. Abbott et al. (1974) recently obtained limited mixing profile probe measurements in a chemically reactive, particle-laden confined jet. Detailed mixing data for particle-laden confined, coaxial jets have not been generally available, however.

Test Facility and Instrumentation

A schematic of the experimental test section is presented in Figure 1. The 2.54-cm diameter primary jet was composed of a two-phase mixture of helium, air, and finely divided aluminum powder. The primary air could be electrically heated to approximately 800°K. The 12.7-cm diameter secondary jet consisted of unheated air. Inlet flow of the two coaxial, concentric jets was parallel. The facility was designed to collect radial profile data at various axial locations. A transparent plastic mixing test section slid over the steel secondary-primary duct assembly permitting the instrument collar to be positioned from near the primary exit to 102 cm downstream of the jet exit plane.

Gas and particle samples were taken with isokinetic collection probes, and gas velocities were obtained from the measured stagnation and static pressures. Eight collection and eight stagnation pressure probes were located so that radial profile data were obtained in two normal planes across the duct. A probe for gas and particle collection was located on the centerline. A stagnation probe for velocity measurements was located near the centerline. Centerline velocities were obtained by extrapolation of an empirical radial profile curve. In order to determine axial profiles, tests were made with the instrument collar at axial locations of 12.7, 25.4, 50.8, 76.2, and 101.6 cm from the jet exit. Helium composition was determined by thermal conductivity analysis (Rush and Forestall, 1947) while particle mass flux was determined from the time required for collection of a weighed particle sample. Pressure and temperature instrumentation, together with the throat areas of choked control nozzles, established the gas flow rates of the primary and secondary jets. The particle feeder was calibrated and pre-set for each test.

Test Conditions

The secondary jet operated near ambient pressure with velocities up to 122 m/s. The primary jet velocity was near 300 m/s for all tests. The extent of helium dilution and air heating was adjusted to achieve a variation in primary jet density of 4/1. The four jet test conditions selected (designated A, B, C, and D) are summarized in Table 1. Tests were run without particles and with 6 μm (Alcan Metal Particles M.D.X.-65), and 30 μm spherical, aluminum particles (Alcan Metal Particles M.D.X.-85-1). The size distributions for these test particles have been reported elsewhere (Hedman, 1973).

Data Reduction

To minimize the errors introduced by jet and instrument collar misalignment and other data scatter, the radial mixing data were statistically correlated to an empirical curve using nonlinear least-squares techniques. The empirical curve also permitted extrapolation of the gas velocity data to the centerline. The following profile was applied to the gas composition, gas velocity, and particle mass flux radial profile data:

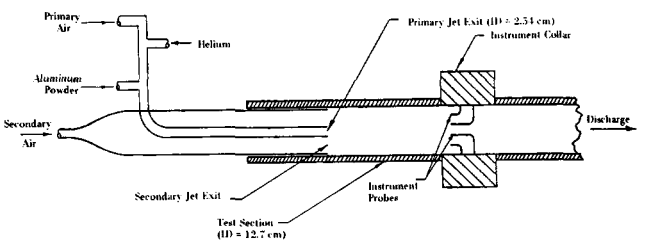

Fig. 1. Schematic diagram of coaxial jet facility test section.

TABLE 1. AVERAGE PRIMARY AND SECONDARY JET CONDITIONS

Parameter, units	Condition A		Condition B		Condition C		Condition D	
	Pri.	Sec.	Pri.	Sec.	Pri.	Sec.	Pri.	Sec.
Velocity, m/s	297	30.8	304	121	273	31.4	279	122
Stagnation temp., °K	487	276	483	258	284	277	286	266
Mass flow rate, kg/s								
Total, gas and powder	0.0516	0.425	0.0521	1.80	0.200	0.423	0.201	1.78
Air	0.0316	0.425	0.0320	1.80	0.157	0.423	0.159	1.78
Helium	0.0100	—	0.0101	—	0.0024	—	0.0024	—
Particles	0.0100	—	0.0100	—	0.0400	—	0.0400	—
Sec./pri. gas flow ratio	10.2		42.8		2.65		11.1	
Sec./pri. gas velocity ratio	0.103		0.398		0.115		0.436	
Sec./pri. gas density ratio	4.38		4.66		1.12		1.18	

$$(G - G_b)/(G_c - G_b) = \exp\left[-\lambda(r^2 - r_i^2)/(r_5^2 - r_i^2)\right] \quad (1)$$

An example of the correlation between the empirical curve and gas velocity test data is shown in Figure 2 (test condition D, 50.8 cm axial location, 6 μm particles). The multiple data points from the probes at 1.7 and also at 3.8 cm where data were reproduced, give an indication of only slight assymmetry in the test-mixing section. Similar agreement was obtained between the empirical curve and gas composition and mass flux radial profile data (Hedman, 1973).

The curve-fitted radial profiles obtained for gas composition, gas velocity, and particle mass flux were used for basic data comparisons. Figure 3 illustrates the radial helium composition profiles (test condition D, 6 μm) obtained at axial locations of 25.4, 50.8, 76.2, and 101.6 cm.

Similar Particle Mass Flux Radial Profiles

The concept of similar profiles is widely accepted in both boundary layer (Schlichting, 1960) and jet mixing studies (Abramovich, 1963). Previous data have shown that similar profiles exist for both composition and velocity (Chriss, 1968). Figure 4 presents the reduced particle mass flux radial profile data for all 6 and 30 μm particle tests at all axial and radial positions normalized as a function of r/r_5. These data normalized in this manner follow a similar profile and the empirical function chosen adequately represents that profile. Agreement was also obtained for both the gas composition and gas velocity similar profiles (Hedman, 1973).

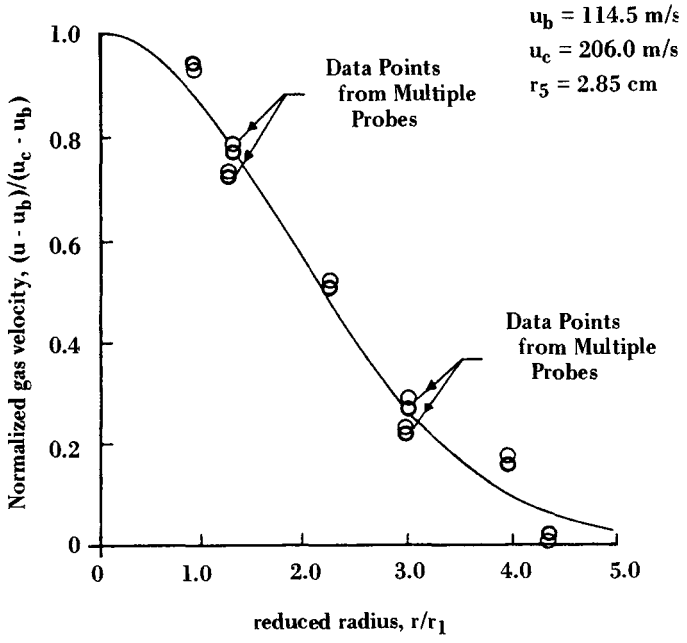

Fig. 2. Comparison of empirical curve fit equation and gas velocity data (D, 50.8 cm, 6 μm aluminum).

Analysis Approach

Mixing characteristics of these confined jets have been evaluated from analysis of the centerline axial decay of gas composition, particle mass flux, and gas velocity. (Tufts and Smoot, 1971; Stowell and Smoot, 1973). Centerline comparisons of particular interest include: (1) the effect of particle size on particle mixing rate, (2) the effect of particles on helium and gas velocity mixing rates, (3) the effect of test

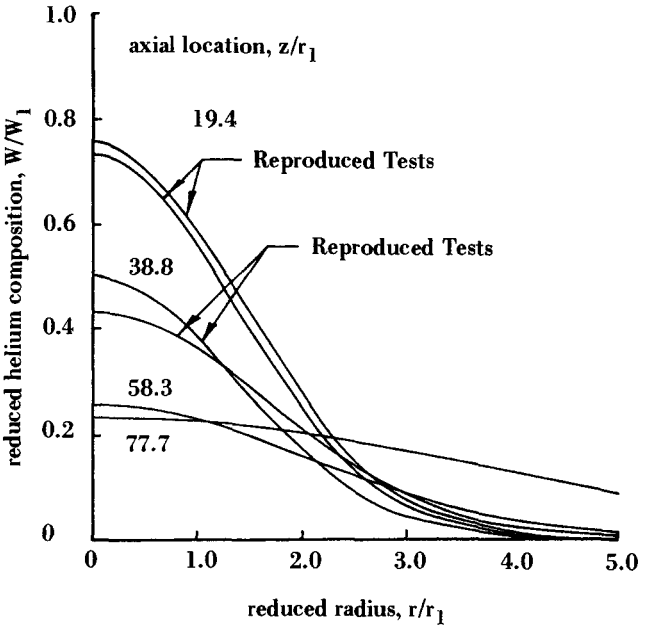

Fig. 3. Normalized helium composition radial profiles for test condition D with 6 μm aluminum powder.

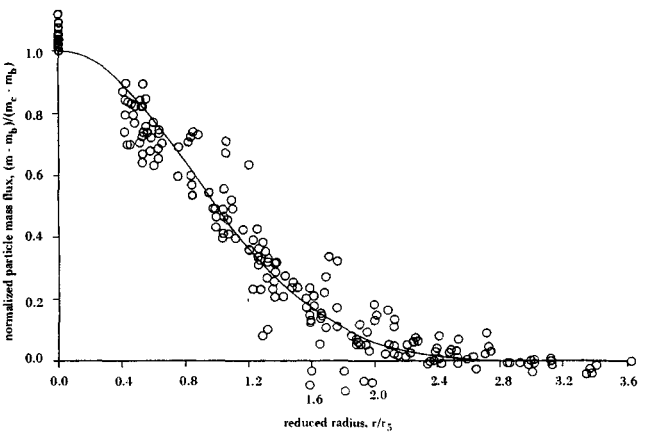

Fig. 4. Similar profile particle mass flux data comparison.

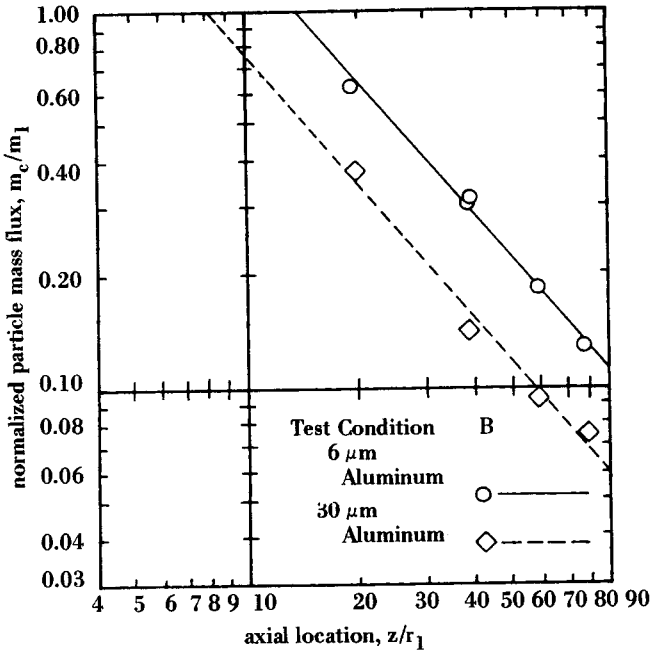

Fig. 5. Experimental particle mass flux centerline decay for 6 and 30 μm aluminum powders.

condition on the mixing rates of helium, velocity, and particle mass flux and (4) the relative mixing rates of the helium, velocity, and particle mass flux for a given test condition. In each figure, the centerline data have been fit by a least-squares technique to the following function which gives a straight line on the log-log plot:

$$\ln Y = A + B \ln (z/r_1) \qquad (2)$$

where

$$Y = m_c/m_1, \quad (u_c - u_b)/(u_1 - u_b), \quad \text{or} \quad W_c/W_1$$

and A and B are correlative constants.

Stowell and Smoot (1973) have shown that a logarithmic line is a good representation of the decay rate for an extensive number of free and confined jet tests. This linear line helps in the data interpretation and makes direct comparison easier. No attempt has been made to report core length, slope, or other mixing coefficient correlation information from these lines. The data have been used to establish the validity of the theoretical model predictions and to determine the relative effects of the test variables.

Particle Effects on Mixing Rates

A comparison of the particle centerline decay for 6- and 30-μm particles is shown in Figure 5 for test condition B. Similar results were seen for the other test conditions. A surprising observation is seen on this figure. The 30-μm particles mixed more rapidly than did the 6-μm particles. If the particle dispersion mechanism were controlled by drag or turbulent diffusion mechanisms, the 30-μm particles would be expected to mix more slowly than would the 6-μm particles. An independent test program conducted at the conclusion of this study (Allred, 1974) suggested that the 30-μm particle velocity substantially lagged that of the gas at the primary nozzle exit plane, causing the particles to disperse more rapidly. The velocity lag of the larger particles was caused by the fine-mesh screens near the exit of the primary jet, resulting in an acceleration of the gas that the particles could not match. A comparison of the 30 μm particle data at all four test conditions showed that the 30-μm particle mixing rate was essentially independent of the test condition (Hedman, 1973). This evidence supports the conclusion that the 30-μm particle decay was being controlled by some mechanism other than turbulent mixing processes. Subsequent tests with and without fine-mesh screens near the nozzle exit, and with a longer inlet section, revealed that the 6-μm particles were essentially in dynamic equilibrium with the gases at the exit plane for all test configurations.

Figure 6 shows the influence of the 6- and 30-μm particles on helium centerline decay for test condition B. In general, the effect of the particles on the gas velocity and the gas composition mixing rates was small. Data plots for other test conditions showed the same general trends (Hedman, 1973).

Test Condition Effects on Mixing Rates

Figure 7 represents the particle mass flux centerline decay data for the four test conditions (A, B, C, and D) using 6 μm aluminum particles. Comparing A with C and B with D shows the marked influence of the low density primary on the core length. The core lengths for test conditions A and B (low

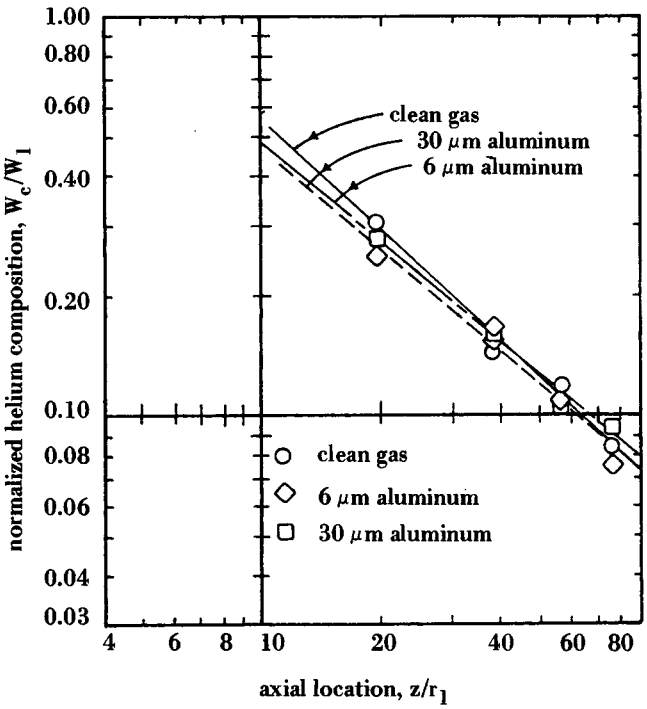

Fig. 6. Effect of powder on helium composition centerline decay for test condition B.

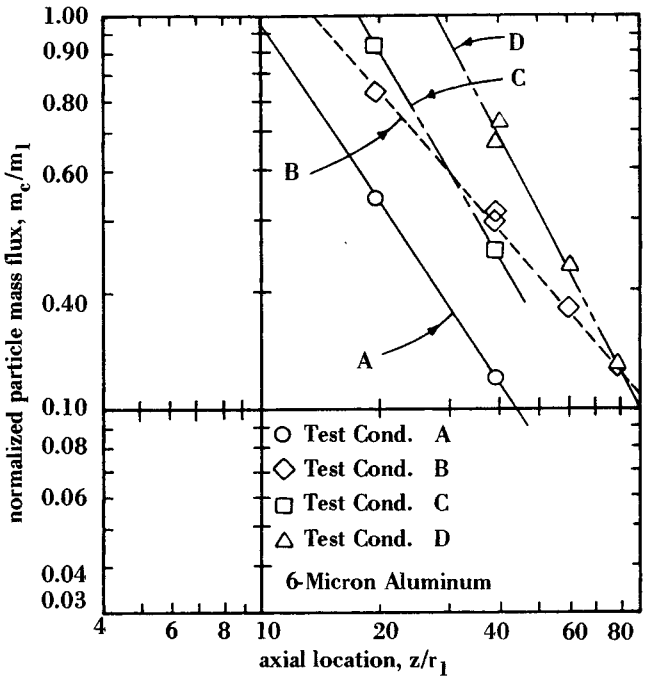

Fig. 7. Effect of test condition on centerline particle mass flux decay (6 μm aluminum powder tests).

density primary) are much shorter (more rapid mixing) than the core lengths of the comparable C and D experiments. A large difference in mixing rate between test condition A and test condition D at a constant secondary to primary gas mass flow ratio is also readily apparent. For these tests, the variation in density had a greater impact on mixing rate than did the variation in secondary velocity. Based on these observations, the relative mixing rates can be ranked as follows:

1. Low velocity secondary and low density primary result in the fastest mixing.
2. High velocity secondary and low density primary result in intermediate mixing rates.
3. Low velocity secondary and high density primary result in intermediate mixing rates.
4. High velocity secondary and high density primary result in the slowest mixing. Similar test condition effects were also seen for the clean gas and 30-μm particle tests (Hedman 1973).

Similar observations resulted for gas velocity data. However, for gas velocity, a change in secondary velocity caused a change in decay slope, while for the 6-μm particles, the change in secondary velocity caused a change in core length.

The effect of test condition on helium composition centerline decay is shown in Figure 8 for the 6μm aluminum test set. This figure indicates that the mixing rate of helium is mostly controlled by the density of the primary stream. Mixing rates for the low density primary tests (A and B) are nearly the same and mixing rates for the high density primary tests (C and D) are also about the same. The differences in mixing rates for low density primary and high density primary are substantial, however. Theoretical predictions shown in Figure 8 are discussed in a later section.

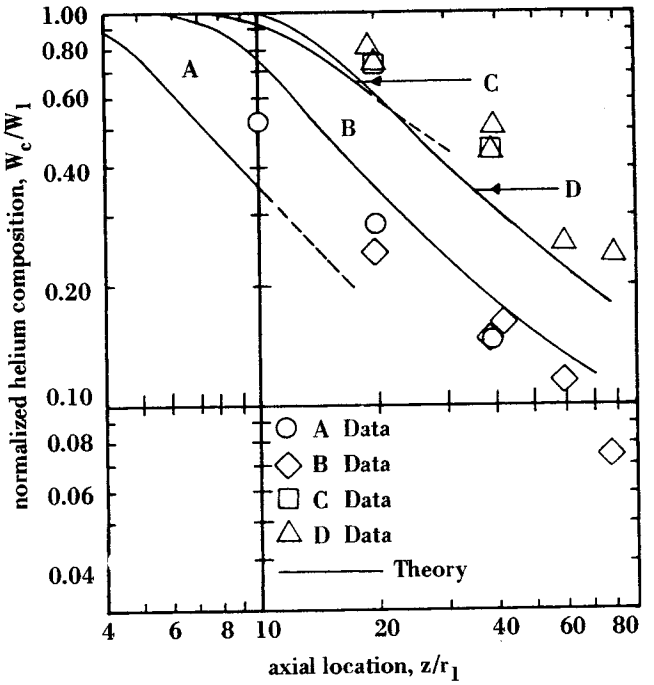

Fig. 8. Comparison of predicted and measured effects of test condition on centerline helium composition decay (6 μm aluminum powder tests).

THEORETICAL MODEL DEVELOPMENT

Literature Review

An earlier study of jet mixing (Smoot et al., 1969 and 1970) included a review of theoretical models available at that time for the mixing and combustion of free and confined, gas-only or particle-laden streams. More recent theoretical work was summarized by Hedman (1973). The models of Cohen (1966) and of Edelman and Fortune (1968) considered nonequilibrium effects of specific gaseous systems. A treatment of Peters (1969) for gaseous mixing in a confined duct employed an integral solution.

Of the models that have been reviewed which treat mixing of primary and secondary streams in a confined duct, few are specifically applied to mixing and/or combustion of particle-gas streams. The work of Channapragada et al. (1967) treats particle-gas mixing with dynamic nonequilibrium. The Baronti and Ferri model (1968) considers the response of the particles to the turbulent fluctuations in the surrounding medium. Edelman and Weilerstein (1969, 1971) have developed a numerical solution to the viscid-inviscid equations for a reactive, multicomponent, coaxial jet system with a condensed phase. The model is restricted, however, to two limiting particle cases: particles in dynamic and thermal equilibrium with the gas phase, and particulate matter uncoupled from the gas-phase plume structure. The earlier models developed by Smoot et al. (1969, 1970) consider general, combusting, gas-particle systems. In addition, these models have treated ignition and extinguishment of the metal particles and nonequilibrium particle effects (Smoot and Anderson, 1971) using an uncoupled solution technique.

Approach

The model developed during this study predicts the mixing characteristics of a particle-laden, confined, coaxial jet with coupled dynamic and thermal nonequilibrium effects. Effects of chemical reaction were not considered.

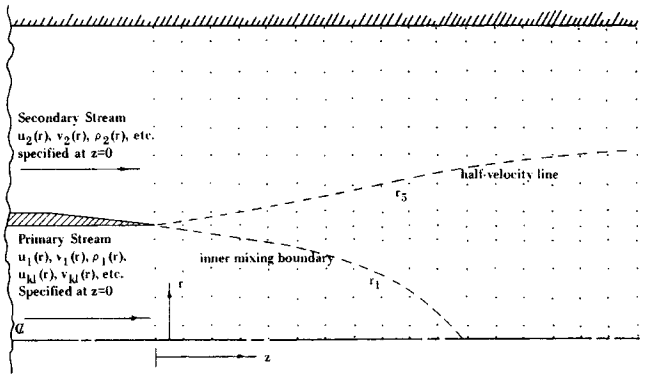

Fig. 9. Configuration of parallel flow confined jet mixing model.

A survey of available finite-difference techniques for treating problems of this type was conducted (Hedman, 1973). The numerical method chosen was that of Keller and Cebeci (1970 and 1971).

A schematic of the flow geometry is presented in Figure 9. The mixing occurs in the region downstream of the primary jet exit plane. The initial conditions at the primary nozzle exit ($z = 0$) are specified for both the primary and secondary streams, but need not be uniform. The flow field is divided into an axisymmetric mesh of grid points. The field of grid points need not have uniform spacing but must have points along the centerline, at the primary jet lip radius (a point of low discontinuity), and at the secondary duct wall.

Figure 9 indicates the boundary location of a constant property core region r_i and location of the locus of half velocity points within the mixing region r_5. These two radii are required in the turbulent eddy viscosity model used, and their definition has an impact on the predicted results.

Equations

The major assumptions used in developing the model are summarized in Table 2. The basic conservation equa-

tions (continuity, motion, and energy) for the general case of a reacting, gas-particle mixture were discussed previously by Smoot et al. (1969). These general equations were simplified to correspond to the specific case studied herein and are summarized in axisymmetric coordinates in Table 3.

The numerical scheme requires that all equations be first order. This has required the introduction of conventional flux terms in order to reduce the second-order terms to first order in the particle continuity, motion, specie conservation, and energy equations (Hedman 1973).

Baronti and Ferri (1968) show the following turbulent continuity equations for the ith gaseous specie and the kth particle phase, respectively:

$$\partial(r\rho_i u_i)/\partial z + \partial(r\rho_i v_i)/\partial r = \partial(r\overline{\rho_i' v_i'})/\partial r \quad (11)$$

$$\partial(r\rho_k u_k)/\partial z + \partial(r\rho_k v_k)/\partial r = \partial(r\overline{\rho_k' v_k'})/\partial r \quad (12)$$

The following condition then results from the requirement of total continuity:

$$\sum_i \overline{\rho_i' v_i'} + \sum_k \overline{\rho_k' v_k'} = 0 \quad (13)$$

The turbulent diffusion terms for the individual gas and powder specie equations are then evaluated from the laminar analog terms:

$$\overline{\rho_i' v_i'} = (\mu/\rho)\partial\rho_i/\partial r \quad (14)$$

$$\overline{\rho_k' v_k'} = (\mu_k/\rho_k)\partial\rho_k/\partial r \quad (15)$$

The model developed during this research program included the particle diffusion term in the particle continuity equation but neglected the corresponding term in the gas continuity equation.

The above system of partial differential equations requires the ideal gas law and several other auxiliary equations which define and relate the required physical variables, the aerodynamic drag forces, the rate of heat exchange between the particles and the gas, and the eddy diffusivity (or eddy viscosity) of the gas and powder phases. Particle drag and heat transfer expressions were obtained from Bird et al. (1960) and Kendall (1962). The gas-phase eddy viscosity expression was taken from the recent work of Stowell and Smoot (1973). A relationship used for the particle-phase eddy viscosity was that of Longwell and Weiss (1953). For the 6-μm particles, this expression gave essentially that of the gas phase. For the 30-μm particles, values were apparently much too small. These auxiliary equations used are reported in detail elsewhere (Hedman, 1973).

Table 2. Coaxial Jet Model Assumptions

- Steady state, boundary layer assumptions valid.
- Axisymmetric geometry, no wall boundary layer effects.
- Nonreactive, two-component, ideal gas phase.
- Constant pressure, molecular and thermal diffusion neglected.
- Single, uniform, spherical particle base treated as continuous medium.
- Particle volume negligible, no particle-particle interaction.
- Gravity effects neglected.
- Turbulent mixing of primary and secondary streams.
- Thermal and dynamic nonequilibrium exists between particles and gas.
- Smoot and Purcell (1967) gas-phase eddy viscosity model.
- Stowell and Smoot (1973) gas-phase turbulent mixing coefficient.
- Longwell and Weiss (1953) particle-phase eddy viscosity relationship.

Solution Technique

The 15 partial differential equations and other auxiliary equations were formulated, cast into finite difference form using a four-point, box scheme (Keller and Cebeci, 1971), and solved into simultaneous algebraic expressions using Newton's method. The system of equations was solved in an iterative manner using a matrix factorization technique (Isaacson and Keller, 1966). The entire system of equations is very lengthy and reported in detail elsewhere (Hedman, 1973).

Each first-order partial differential equation requires a boundary condition. The model assumptions shown in Table 2 provide these conditions. The axisymmetric assumption requires that all flux terms ($\partial u/\partial r$, etc.) be zero on the centerline. Additionally, there can be no radial velocity on the centerline or at the wall (that is, across streamlines). The assumption of no wall boundary layer or other wall effects requires that the flux terms at the wall also be zero.

COMPARISON OF MODEL PREDICTIONS WITH EXPERIMENT

The fully coupled, nonreacting, particle-gas mixing model presented above was used to make theoretical predictions for the clean gas, 6-μm particle tests, and the 30-μm particle tests. Model input parameters were taken from the test conditions reported previously and selected predictions related to these tests were made. Typical comparisons between the model prediction and measurements are shown below. Even though the model predicts the full radial and axial mixing behavior of the jets, the comparisons herein have been limited to the centerline decay comparisons. The predicted radial profiles throughout the

Table 3. Summary of Partial Differential Equations (Smoot et al., 1969)

(a) Gas Phase Equations

Continuity:	$\partial(\rho u)/\partial z + (1/r)\partial(r\rho v)/\partial r = 0$	(3)
z-motion:	$\rho u\partial u/\partial z + \rho v\partial u/\partial r = (1/r)\partial[(\mu r\partial u/\partial r)/\partial r] + F_{zk}$	(4)
Primary gas specie:	$\rho u\partial W/\partial r + \rho v\partial W/\partial r = (1/r)\partial[(\mu r/Sc)\partial W/\partial r]/\partial r$	(5)
Energy:	$\rho u\partial H/\partial z + \rho v\partial H/\partial r = (1/r)\partial[(\mu r/Pr)\partial H/\partial r]/\partial r + u_k F_{zk} + Q_k + (1/r)(1 - 1/Pr)\partial[\mu r\partial(u^2/2)/\partial r]/\partial r$	(6)

(b) Particle Phase Equations

Continuity:	$\partial(\rho_k u_k)/\partial z + (1/r)\partial(r\rho_k u_k)/\partial r = (1/r)\partial[(r\mu_k/\rho_k)\partial\rho_k/\partial r]/\partial r$	(7)
z-motion:	$\rho_k u_k\partial u_k/\partial z + \rho_k v_k\partial u_k/\partial r = (1/r)\partial(\mu_k r\partial u_k/\partial r)/\partial r - F_{zk}$	(8)
r-motion:	$\rho_k u_k\partial v_k/\partial z + \rho_k v_k\partial v_k/\partial r = \partial[(\mu_k/r)\partial(rv_k)/\partial r]/\partial r - F_{rk}$	(9)
Energy:	$\rho_k u_k\partial H_k/\partial z + \rho_k v_k\partial H_k/\partial r = (1/r)\partial(\mu_k r\partial H_k/\partial r)/\partial r - u_k F_{zk} - Q_k$	(10)

mixing region were in good agreement with those observed experimentally (Hedman, 1973).

Effect of Test Condition

Figure 8 compared predicted and measured helium centerline profiles. Both the magnitudes of the measured composition and the effect of test condition are quite well predicted. The general order of mixing rates is also predicted: A > B > C > D.

Effect of Particle Diffusion

Theoretical predictions were made both with and without the particle eddy diffusion term (that is, with $\mu_k = 0$ and $\mu_k \neq 0$) included in the particle continuity equation. In both cases, the model predicted the correct behavior of the gas composition and gas velocity. However, the predicted particle diffusion rates for the case where the particle diffusion term was not included were very much less than that observed experimentally. With inclusion of the particle diffusion term in the particle continuity equation, good agreement resulted between the observed 6-μm particle mixing rates and that predicted by the model results. The magnitude of the particle eddy viscosity was comparable to that of the gas. The eddy diffusion term in the particle continuity equation is a dominant term and must be considered. For the tests considered herein, turbulent mixing rather than mean aerodynamic drag, dominates the particle dispersion. The predictions presented below include the particle diffusion term.

Eddy Viscosity Model

The gas phase eddy viscosity expression used in this jet mixing model (Stowell and Smoot, 1973) requires the specification of the inner mixing boundary. The practice used was to select the radius that corresponds to a prescribed dimensionless velocity value U_i along the inner mixing boundary. The selection of this value U_i is not completely arbitrary but should correspond to the definition used in deducing the mixing coefficient. This would ensure that the mixing coefficient correlation used is consistent with the prediction being made. The value of U_i should be near unity. In most of the predictions below, a value of 0.85 for U_i was selected.

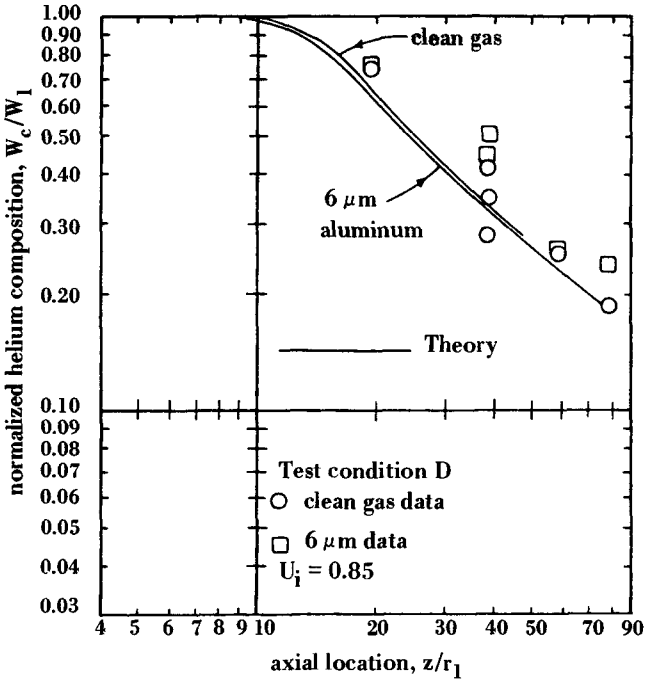

Fig. 10. Comparison of predicted centerline helium composition decay with experiment-test condition D, clean gas and 6 μm aluminum powder.

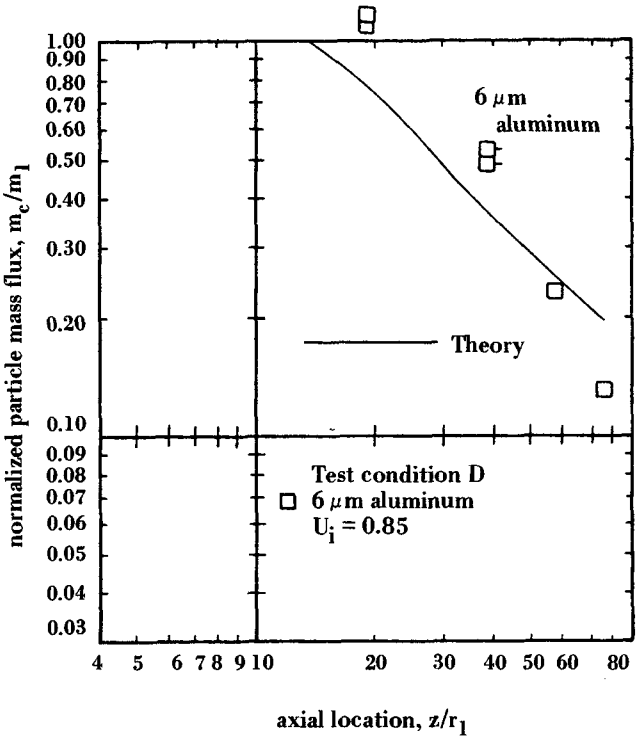

Fig. 11. Comparison of predicted centerline particle mass flux decay with experiment-test condition D, 6 μm aluminum powder.

Clean Gas and Six-Micrometer Aluminum

Comparisons between the theoretical model predictions and the test data for clean gas and 6-μm aluminum powder centerline decay data are presented in Figure 10 and 11 for helium composition and particle mass flux, respectively. Similar comparisons were also made for gas velocity. The predicted mixing rate was somewhat faster than those observed for the helium, velocity, and powder. The predicted slope in the decay region for the helium composition and gas velocity are approximately correct. The predicted slope for the particle mass flux is too low.

Within the accuracy of the data, there was little or no observed effect of the particles on the mass or momentum mixing rates. The results from the theoretical predictions also indicate a small but predictable effect. Figure 10 shows that the presence of the 6-μm aluminum powder theoretically causes the helium composition mixing to be slightly more rapid. The effect of the particles on the velocity was also slight and is mostly accountable from the particle drag effects. Centerline decay comparisons for the other test conditions were made (Hedman, 1973) with similar results.

Thirty-Micrometer Aluminum

Based on theoretical considerations, it was expected that the 30-μm aluminum powder would mix much more slowly than the 6-μm powder. The actual mixing rate observed for the 30-μm powder was, however, much more rapid than expected and generally more rapid than that observed for the 6-μm powder (Hedman, 1973). Allred (1974) showed that the excessive particle velocity lag in the 30-μm powder at the primary jet exit was primarily responsible for the very rapid mixing observed for these larger particle sizes. Model predictions demonstrated that the magnitude of the initial particle velocity lag had a

very significant effect on the 30-μm powder mixing rate (Hedman, 1973). These results also suggest that the magnitude of 30-μm particle eddy viscosity was comparable to that for the gas phase.

ACKNOWLEDGMENT

This work was sponsored by the Power Program, Office of Naval Research, Washington, D.C.

NOTATION

F_{zk} = kth particle axial drag force, N/m^3
F_{rk} = kth particle radial drag force, N/m^3
G = general property (U, m, W)
H = stagnation enthalpy, J/kg
m = particle mass flux, kg/m^2-s
Pr = turbulent Prandtl number
Q_k = convective rate of heat addition from particle to gas per unit volume, J/m^3-s
r = radial coordinate, m
Sc = turbulent Schmidt number
u = axial velocity, m/s
U = reduced gas axial velocity, $(u - u_2)/(u_1 - u_2)$
v = radial velocity, m/s
v' = fluctuating component of radial velocity, m/s
W = weight fraction of primary gas
z = axial coordinate, m

Greek Letters

μ = eddy viscosity, kg/m-s
ρ = density, kg/m-s
ρ' = fluctuating component of density, kg/m-s
λ = ln 2

Subscripts

1 = primary jet exit
2 = secondary jet exit
5 = radial location where property (for example, velocity) is average of centerline and near wall values.
b = limiting value at large radius
c = centerline value
i = gas specie
i = inner mixing boundary
k = particle phase

LITERATURE CITED

Allred, L. D., "Particle and Gas Mixing Effects in Confined, Nonparallel, Coaxial Jets," M.S. thesis, Brigham Young Univ., Provo, Utah (1974).

Abbott, S. W., L. D. Smoot, and K. Schadow, "Direct Mixing and Combustion Efficiency Measurements in Ducted, Particle Laden-Jets," *AIAA J.*, **12**, 275 (1974).

Abramovich, G. N., "The Theory of Turbulent Jets," The M.I.T. Press, Cambridge, Mass. (1963).

Baronti, P. O., and A. Ferri, "Mixing and Combustion of Solid Particles in Turbulent Streams," ATL TR-112, Advanced Technol. Lab., Inc. (1968).

Channapragada, R. S., R. Anderson, R. Duvvuri, and A. Gopalakrishnan, "Mixing, Ignition and Combustion Analysis of Air-Augmented Solid Rockets and Boron Particles," AIAA Paper 67-481, 3rd Propulsion Joint Specialist Conf., Washington, D.C. (1967).

Chriss, D. E., "Experimental Study of Turbulent Mixing of Subsonic Axisymmetric Gas Streams," Report AEDC-TR-68-133, Aro, Inc., Tenn. (1968).

Cohen, L. S., "An Analytical Study of the Mixing and Nonequilibrium Chemical Reaction of Co-flowing Compressible Streams," paper presented at 2nd Propulsion Joint Specialist Conf. of AIAA, Colorado Springs, (1966).

Edelman, R., "Turbulent Transport in Polydisperse Systems," General Appl. Sci. Lab. GASL TR 735 (1973).

———., and O. Fortune, "An Analysis of Mixing and Combustion in Ducted Flows," paper presented at AIAA 6th Aerospace Sci. Mtg., New York (1968).

Edelman, R. B., and G. Weilerstein, "A Solution of the Invisicid-Viscid Equations with Applications to Bounded and Unbounded Multicomponent Reacting Flows," paper presented at AIAA 7th Aerospace Sci. Mtg., New York (1969).

———., "An Analysis of the Moderate Altitude Two-Phase Flow Plume," CPIA Publ. No. 209, JANNAF 6th Plume Technol. Meeting, Naval Postgraduate School, Monterey, Calif. (1971).

Field, M. A., D. W. Gill, B. B. Morgan, and P. G. W. Hawksley, "Combustion of Pulverised Fuel; Part II. Flow Patterns and Mixing," Monthly Bull. Br. Coal Utilisation Research Assoc., **30**, 455 (Nov.-Dec., 1966).

Goldschmidt, V., and S. Eskinazi, "Two-Phase Turbulent Flow in a Plane Jet," *ASME Trans.*, Vol. 33E (1966).

Harsha, P. T., "Free Turbulent Mixing AG: Critical Evaluation of Theory and Experiment," Report AEDC-TR-71-36, Aro, Inc., Tenn., (1971).

Hedman, Paul O'Dell, "Particle-Gas Dispersion Effects in Confined Coaxial Jets," Ph.D. dissertation, Brigham Young Univ., Provo, Utah (1973).

Isaacson, E., and H. B. Keller, *Analysis of Numerical Methods*, Wiley, New York (1966).

Keller, H. B., and T. Cebeci, "Accurate Numerical Methods for Boundary Layer Flow-I. Two Dimensional Laminar Flows," Lecture Notes in Physics, Proc. Second Intern. Conf. on Numerical Methods in Fluid Dynamics, Springer Verlog (1971).

———., "Accurate Numerical Methods for Boundary Layer Flows-II. Two Dimensional Turbulent Flows," paper presented at AIAA 9th Aerospace Sci. Mtg. (1971).

Kendall, R. M., "The Real Gas, Two Phase Flow Expansion Program," 53/C-TN 36, Vidya Research and Development, Palo Alto, Calif. (1962).

Longwell, J. P., and M. A. Weiss, "Mixing and Distribution of Liquids in High Velocity Air Streams," *Ind. Eng. Chem.*, **45**, 662 (1953).

Peters, C. E., "Turbulent Mixing and Burning of Coaxial Streams Inside a Duct of Arbitrary Shape," paper presented at AIAA 2nd Fluid and Plasma Dynamics Conf., San Francisco (1969).

Pritts, O. R., "Particle Dispersion Study," AFOSR 70-2713 TR, Control No. U-70-26 A, Thiokol Chemical Corp., Huntsville Div., Alabama (1970).

Rush, D., and W. Forstall, "Apparatus for the Determination of the Concentration of Helium in Air by the Thermal Conductivity Method," Meteor Internal Report No. 4, Gas Turbine Lab., M.I.T., Cambridge, Mass. (1947).

Sargent, W. H., K. E. Woodcock, R. S. Anderson, and T. Duvvuri, "Investigation of Air-Augmented Rocket Combustion and Mixing Processes," Air Force Rocket Propulsion Lab., AFRPL-TF-68-88 (1968).

———., "Investigation of Air-Augmented Rocket Combustion and Mixing Processes," *ibid.*, AFRPL-TF-167 (1968).

Schlichting, A., *Boundary Layer Theory*, McGraw-Hill, New York (1960).

Smoot, L. S., and G. S. Anderson, "Particle Nonequilibrium Effects in Mixing and Combustion of Ducted Particle-Laden Flows," presented at AIAA/SAE 7th Propulsion Joint Specialist Conf., Salt Lake City, Utah (1971).

Smoot, L. D., R. L. Coates, and J. M. Simonsen, "Mixing and Combustion of Compressible, Particle-Laden Ducted Flows," paper presented at AIAA 5th Propulsion Joint Specialist Conf., San Diego, Calif. (1970).

Smoot, L. D., and W. E. Purcell, "Model for Mixing of a Compressible Free Jet with a Moving Environment," *AIAA J.*, **5**, 2049 (1967).

Stowell, D. E., and L. D. Smoot, "Rates of Turbulent Mixing in Particle-Laden Combustion Systems," paper presented at AIAA 9th Propulsion Conf., Las Vegas, Nevada (1973).

Tufts, L. W., and L. D. Smoot, "A Turbulent Mixing Coefficient Correlation for Coaxial Jets with and without Secondary Flows," *J. Spacecraft Rockets*, **8**, 1183 (1971).

Manuscript received September 30, 1974; revision received December 30, 1974, and accepted January 2, 1975.